Colloid Polym Sci (2009) 287:203–214
DOI 10.1007/s00396-008-1967-y

ORIGINAL CONTRIBUTION

Gd^{3+} binding of carboxylated polyglycidyl methacrylate latices and their colloidal stability

S. Schumacher · R. Wüstneck · B.-R. Paulke · R. Cartier · U. Pison

Received: 15 August 2008 / Revised: 13 October 2008 / Accepted: 6 November 2008 / Published online: 27 November 2008

Abstract The binding of Gd^{3+} to two carboxylated polyglycidyl methacrylate latices was investigated. The latices differed in size (60 and 140 nm for CL6 and CL3, respectively) and surface charge density. The Gd^{3+} concentration in aqueous suspension was determined using an arsenazo (III) assay. Using $^{153}Gd^{3+}$, the bound amount was determined directly. Because of the high binding affinity, ligand depletion became evident. The binding was pH dependent, investigated in buffer solutions not influencing the arsenazo (III) assay. Optimal binding occurs by formation of sodium salts of the carboxylic groups and replacement of Na^+ and H^+ by Gd^{3+}. The dissociation constants of the particles were $k_D \approx 5 \times 10^{-5}$ mol/L (CL3) and 10^{-4} mol/L (CL6), without cooperativity (Hill plot). Colloidal stability was investigated.

Electronic supplementary material The online version of this article (doi:10.1007/s00396-008-1967-y) contains supplementary material, which is available to authorized users.

S. Schumacher
Fraunhofer Institute for Biomedical Engineering IBMT,
Potsdam, Germany

R. Wüstneck (✉) · U. Pison
Clinic for Anaesthesiology and Intensive Care Medicine,
Charité Campus Virchow-Klinikum, Berlin University Medical School,
Berlin, Germany
e-mail: rainer.wuestneck@gmail.com

B.-R. Paulke
Water-based Polymer Systems, Fraunhofer Institute for Applied Polymer Research,
Potsdam, Germany

R. Cartier
Pharmaceutical Nanotechnology,
Boehringer Ingelheim Pharma GmbH & Co. KG,
Ingelheim am Rhein, Germany

Keywords Gadolinium · Binding · Polyglycidyl methacrylate nanoparticles · Ligand depletion · Colloidal stability

Introduction

Nanoparticles carrying superparamagnetic metal ions are employed to enhance the contrast in magnetic resonance imaging (MRI) by shortening the longitudinal and transversal spin–spin relaxation times (T_1, T_2) of protons [1]. Gadolinium (III) chelates, such as diethylenetriaminepentaacetic acid (DTPA) and others, are the predominant contrast agents in commercial use (Magnevist®, Eovist®, Omniscan®, ProHance®, etc.) [2]. Chelates have the advantage of realizing a strong Gd binding and of being hydrophilic. Therefore, chelates are not expected to enter cells and to interact with DNA [2]. Chelates are known to penetrate unspecifically into tissue, which is sometimes a disadvantage. The usage of Gd bound to DTPA, however, is not the only possible way to apply the highly toxic Gd^{3+} in secure medical use [3, 4]. Recently, we presented results showing that carboxylated polyglycidyl methacrylate latices (P-EPMA) can be used as functionalized nanocarrier systems and MRI contrast-enhancing agents, whereas the amount of Gd^{3+} injected into the body can be reduced even with enhanced MRI contrast in comparison to Magnevist® [5]. Furthermore, we demonstrated that the same P-EPMA nanoparticles modified by ^{68}Ga or ^{111}In could be used in scanning heart and liver or for gamma scintigraphy, respectively. Therefore, it is worth characterizing the binding behavior of P-EPMA nanoparticles for heavy metal ions in more detail, to optimize the binding, and to compare the impact of different P-EPMA particles in enhancing MRI contrast.

The present paper presents some essential prerequisites to optimize Gd^{3+} binding to carboxylated P-EPMA particles, thus preparing in vivo testing of these particles. Results characterizing the MRI contrast-enhancing capacity of these particles will be published separately. The particles used were modified by incorporation of rhodamine B. In our previous paper [5], such labeling was used for flow cytometry to demonstrate association of nanoparticles with different cells. In the present paper, rhodamine B labeling is used to qualitatively check the efficiency of some procedures of particle detaching qualitatively, i.e., centrifugation and ultrafiltration. Similar particles were studied by us recently [6].

The aim of the present paper is

- to characterize and test two synthesized P-EPMA nanoparticles which differ in diameter, core-to-corona ratio, and density of negatively charged groups,
- to work out the conditions to perform reliable binding experiments,
- to characterize the Gd^{3+} binding to the particles by using two independent methods that determine both the bound and the free Gd^{3+} ions in water and physiological buffer solutions,
- to determine the binding constants, and
- to characterize the range of colloidal stability of the two Gd^{3+} modified P-EPMA nanoparticles.

Finally, conditions will result which allow the preparation of Gd^{3+}-modified particle suspensions which are suitable for testing contrast-enhancing properties by MRI. Such particles should be modified by antibodies to realize directed targeting in further stages of particle development.

Materials and methods

Gd^{3+} ion binding was determined by using both the arsenazo (III) assay [7] to determine the concentration of free Gd^{3+} in solutions and $^{153}Gd^{3+}$ to determine the amount of Gd^{3+} bound by particles directly. Arsenazo (III) ((2,2′-(1,8-dihydroxy-3,6-disulfonaphthylene-2,7-bisazo)dibenzenearsonic acid), $GdCl_3$, Tricine (*N*-(2-Hydroxy-1,1-bis (hydroxymethyl) ethyl)glycine), Tris(HCl) (Tris(hydroxymethyl)-aminomethan), HEPES (4-(2-hydroxyethyl)-1-piperazin ethansulfonic acid), rhodamine B, potassium peroxydisulfate methacrylic acid, and 2,3-epoxypropyl methacrylate were obtained from Sigma Aldrich, Seelze, Germany and $^{153}GdCl_3$ from Perkin Elmer LAS (Germany) GmbH. SDS was obtained from SERVA, Germany.

All chemicals were used as received. The solutions were prepared with ultra-pure water from a Millipore unit. This water was also used in the ultrafiltration process for latex purification.

Nanoparticle preparation was described previously [5].

Briefly, "hairy" particles, carboxylated polyglycidyl methacrylate latices, were synthesized by semi-batch emulsion copolymerization in a 250-mL double wall glass reactor (HWS Mainz), equipped with glass anchor stirrer, nitrogen inlet, reflux condenser, and dropping funnel. For latex CL 3, 0.2 g sodium dodecyl sulfate (SDS) was dissolved in 156 mL water; for latex CL 6, 0.7 g SDS was used. For both lots, 0.108 g potassium peroxydisulfate dissolved in 20 mL ultra-pure water was applied as initiator solution. The SDS amount in water for latex CL 3 [3.54 mmol/L in reactor fleet], supplemented by 20 mg rhodamine B, was placed in the reactor. The same was done with the SDS solution for CL 6 [12.4 mmol/L in reactor fleet]. Eighteen grams of 2,3-epoxypropyl methacrylate [0.65 mol/L] was added for CL 3, 4.0 g for CL 6. The emulsion was purged with nitrogen under stirring (350/min) for 20 min at ambient temperature. Then, while heating up to polymerization level (60 °C), purging with nitrogen was continued. The potassium peroxydisulfate solution was poured into the dropping funnel. An amount of 1.6 g for CL 3 and 1.2 g for CL 6 of the carboxylating agent, methacrylic acid, was dissolved in ultra-pure water and filled up with it to a total volume of 20 mL [0.095 mol/L in reactor fleet]. This solution was sucked into a 20-mL plastic syringe (B. Braun) which was fixed on an infusion pump (type 610 B.S., Medipan Warszawa). After 10 min at 60 °C, the polymerization was started by fast inflow of the potassium peroxydisulfate solution from the dropping funnel into the monomer emulsion in the reactor [2.04 mmol/L in reactor fleet]. At the same time, the infusion pump was started. Over a period of 2.2 h, it admixed the methacrylic acid solution constantly to the polymerizing latex. After 6 h, the polymerization was finished by stopping the nitrogen stream and cooling down the latices. The results were polymer dispersions with solid contents of approximately 10% for CL 3 and 3.2% for CL 6.

Purification of the latices was performed in two steps. The first was dialysis of 100-mL latex, each against 3–5 L deionized water. The exclusion limit of the dialysis tubes was 14,000 Da. The water was changed twice a day. For the next step, the 100-ml latex portions were diluted with ultra-pure water to 400 mL and filled into ultrafiltration cells of this volume equipped with suitable track-etched membranes (100-nm pore diameters for CL 3 and 25-nm pore diameters for CL 6). The process was controlled by measuring the electrical conductivity in the aqueous filtrate. At a value of 1 μS/cm in the filtrate, the purification process was stopped. More details have been described in [8]. All molar data are related to 196 mL total water volume in the reactor.

Binding experiments were carried out under saturation conditions. For binding experiments using the arsenazo (III)

assay, 1,000 μL $GdCl_3$ solutions of different concentrations were added dropwise to 1 mg/mL particle suspensions with intensive stirring. After 30-min incubation, CL3 particles were separated by centrifugation (19,800 ×*g* at 21 °C), whereas the CL6 particles were separated by ultrafiltration (Vivaspin 2, PES membrane, 100 kDa, Sartorius). To these solutions, 500 μL of 0.2 mM arsenazo (III) was added and the absorption at λ=654 nm was determined (Beckmann DU640). Bound Gd^{3+} was determined by the difference between the Gd^{3+} concentration in the supernatant solution and the total amount of Gd^{3+} added. In cases of the use of buffer solutions, a double concentrate was added to a corresponding suspension in water. Saturation experiments using $^{153}Gd^{3+}$ were carried out by dropwise addition of 250 μL $^{153}GdCl_3$ solutions in Tricine buffer to the particle suspension (250 μL, 1 mg/mL, pH=7.2). After 30-min incubation, the particles were separated by centrifugation (Nanosep Centrifugal Devices from Pall Life Science, polyethersulfone membrane on polyether substrate, 100 μL, 30 min at 600 ×*g*). Radioactivity of the supernatant solution was determined using a 1480 Wallac WIZARD™. The amount of unbound Gd^{3+} was determined by washing the filter with 500 μL Tricine buffer.

Particle size, polydispersity index, and electrophoretic mobility were determined by dynamic light scattering using a Nano-ZS Zetasizer and a ZetaMaster (Malvern Instruments, Herrenberg, Germany). For a photochemical assay (Arsenazo (III), a DU 640 photometer was used (Beckmann, Germany). Radioactivity was measured in a 1480 Wallac WIZARD™ gamma counter (PerkinElmer, Rodgau-Jügesheim, Germany).

Results and discussion

Characterization of P-EPMA particles

The aim of particle synthesis was to obtain "hairy" model P-EPMA nanoparticles with different diameter, charge, and core/corona ratio to change body localization and residence time. Firstly, 140-nm-sized particles were chosen to bind Gd^{3+} (CL3). Such particles are known to accumulate in the liver when injected intravenously [9]. Secondly, smaller particles (CL6) were synthesized to reach organs other than the liver. To increase the contrast of a special organ, a particle size of about 60 nm was chosen, as particles of such size are believed not to spill over uncontrolled [10]. The EPMA/MAA ratio was changed in order to guarantee an adequate density of carboxyl groups, if the smaller particles are used. It was 2:1 for CL6 in contrast to 7:1 for CL3.

The size of the particles was determined using dynamic light scattering. The average particle sizes are given in Table 1. The particle sizes of CL3 and CL6 in water meet the objective of particle synthesis.

Furthermore, the influence of buffer solutions and pH on the particle size was tested. The physiological Tricine buffer was chosen, as this buffer meets the analytical demands, as will be shown below. For the CL3 particles in Tricine buffer and for different pH, no significant changes in the average size were established. In contrast, the size of CL6 was influenced by the presence of Tricine buffer as well as by changes in pH, which indicates different corona properties of the two particles.

The dynamic light scattering technique requires low particle concentrations. Routinely, a particle concentration of 0.1% (*w*/*w*) was used. The pH of the CL6 particle solutions at this concentration was about 5 after synthesis and purification procedures. When the pH was shifted to 7.4 by titration with NaOH, the average size increased by about 10 nm. This increase is obviously due to increasing mobility caused by stretching or increase of linear orientation of the MAA chains, whereas mobility was reduced by coiling of the MAA chains in acidic environment. In contrast to this, the presence of 50 mM Tricine buffer decreased the size of the CL6 particles by more than 15 nm, and even by about 20 nm when pH 7.4 was previously adjusted. The latter effect may be explained by the common compression of the electrolytic diffusion layer. Similar small but not significant changes in diameter of the CL3 particles were observed. The polydispersity index, PDI, was small for the particles synthesized. This confirms the quality of synthesis. For the present consideration, it shows that the procedure did not violate the demands of colloidal stability.

Using end-point titration with 0.0001 m poly-diallyldimethyl-ammonium chloride, the charge densities of the particles were determined. The surface charge titration was performed in a Teflon beaker of a particle charge detector (Muetek, Germany), controlled by an automatic titrator

Table 1 Average hydrodynamic particle diameter (d_{av}) and polydispersity index (PDI) determined by dynamic light scattering of the particles CL3 and CL6 in different environments

	CL3		CL6	
	d_{av} nm	PDI	d_{av} nm	PDI
Water pH=5	140.9±2.6	0.067±0.022	74.5±0.5	0.133±0.009
Water pH=7.4	146.3±5.1	0.037±0.020	84.8±1.4	0.143±0.009
Tricine pH=8.15	140.4±2.9	0.008±0.007	56.6±1.1	0.079±0.005
Tricine pH=7.4	137.7±2.8	0.006±0.001	54.7±0.7	0.071±0.008

Tricine buffer 50 mM

(Titrino 316, Metrohm, Switzerland). The streaming potentials of the dispersions were between −1.1 and −1.8 V when tritration started. Taking into account the dispersion density (1.25 g/cm^3 and 1.38 g/cm^3 for CL3 and CL6, respectively), the charge density for the particles could be calculated. The results are collected in Table 2 whereas a rough estimation of the core volume of the particles was obtained by sedimentation analysis of the particles using a Beckmann ultracentrifuge with 35,000 rpm for 40 min which allows a rough estimation of the particle charge density per surface of a solid sphere. Due to the centrifugation force, the hairy structure of the latex collapsed onto the surface of the highly cross-linked shell. A visualization of the particles with shell and core was possible by using AFM; see ESM 2 of the Electronic supplementary material.

The results show that the charge densities determined by end-point titration of both particles nearly agree when considering different particle diameters and densities. The results per gram particle show however the expected gradation. The charge density of 100% sulfate groups at a surface of a smooth sphere would be about 34 μC/cm^2. Therefore, the charge densities calculated by titration cannot be positioned on a smooth surface, i.e., they must be distributed within the hairy corona. When taking into account the core diameters of the particles, the negative charge density of the CL3 particles is about 60% higher than that of CL6, in agreement with the larger surface of one CL3 particle.

Another important aspect of the particle properties is the effect of surface charge on the electrophoretic mobility. We do not give here ζ potential, which is calculated from the electrophoretic mobility. For soft particles with a polyelectrolyte-like shell, the ζ potential becomes less important and, for most cases, loses its physical meaning [11]. Therefore, we prefer to present the surface charge characteristics in the form of the electrophoretic mobility, i.e., the actual measured parameter, because there are no accepted and suitable models to characterize "hairy" particles. To obtain information about particle charge, the electrophoretic mobility was determined for particle suspensions, which were titrated with 0.1 N NaOH and starting in the acidic range (Fig. 1).

Table 2 Charge density of the particles in dispersion calculated by end-point titration and surface charge density estimated by using particle core diameters

	Charge density determined by titration, μC/cm^2	Charge density, C/g particles	Estimated core diameter, nm	Surface charge density, μC/cm^2
CL3	237.54	91.2	81	153.9
CL6	238.45	236	17	92.1

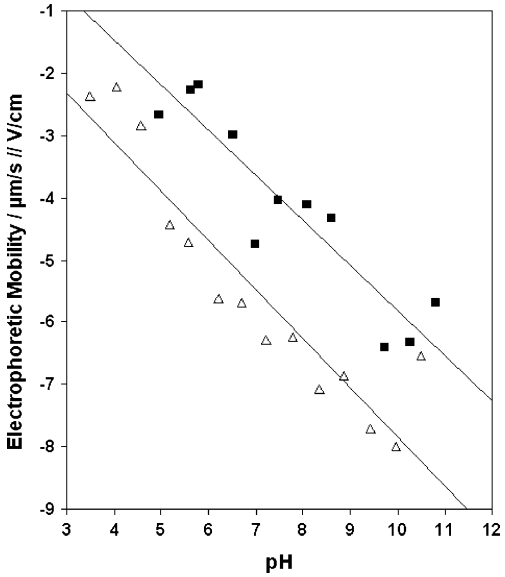

Fig. 1 Electrophoretic mobility versus pH for CL3 (Δ) and CL6 (■). The suspensions 0.01 wt.% CL3 and 0.1 wt.% CL6 were titrated with 0.1 N NaOH. Starting pH was adjusted by addition of 0.1 N HCl, room temperature

The starting pH values were adjusted by addition of 0.1 N HCl. The particle concentrations were chosen in agreement with instrumental conditions, i.e., approx. 0.1% (*w*/*w*) for CL6 and about 0.01% for CL3.

As expected, all mobilities determined are negative, indicating a movement of particles to the anode. The mobilities are relatively low in acidic environment but increase linearly with increasing pH, whereas the mobilities for the CL3 are generally higher, i.e., more negatively charged than the CL6 particles (see Table 2). The linear dependencies versus pH of both particles are nearly parallel, which supports the assumption that both processes can be explained analogously. The differences are clearly determined by the particle properties. As expected from the charge density of the particles, the electrophoretic mobilities for CL3 are higher then those of the CL6 particles. The mobility, however, is influenced by electrical field, environment properties, and the Brownian molecular movement. The effects found can be explained by the 'hairy' character of nanoparticles with different ratios between the cross-linked hard core and a flexible corona of water-soluble polymer chains around. We find nearly identical surface charge densities by titration to the point of zero charge if we look at the colloid as a whole from outside, taking its hydrodynamic diameter from dynamic light scattering as a basis. In the case of CL3, however, the core is dominating the colloidal cross-section, whereas in the case of CL6, we find a dominance of the corona in the internal structure. A sharp differentiation in the charge characteristics of both particles can be seen, if we either relate the number of surface charges found in titration on

the particle mass or on the surface area of the cross-linked core (see Table 2). This graduation is the reason for the behavior of both nanoparticles in the electric field. CL3 colloids demonstrate higher electrophoretic mobility, though CL3 particles have the higher hydrodynamic as well as the higher hard core diameter. We assume that, in an alternating electric field, the attraction force is effective first of all on the charged hard core of a 'hairy' nanoparticle. The corona is following indolently. The presence of a dynamic corona of flexible, water-soluble polymer chains should be primarily reflected by friction effects. This is reflected indeed when comparing electrophoresis data of CL3 and CL6 nanoparticles. The general increase in mobility with increasing pH can be explained by dissociation equilibrium of the carboxylic surface functions in aqueous environment.

Another aspect is the big difference between the particle diameters of both particles. For small particles, the Brownian motion is higher and may reduce the particle flow in an electrical field, which also results in higher mobilities for the CL3 particles.

Binding experiments

Particles and $GdCl_3$ were incubated for 30 min at room temperature. This incubation time was found to be sufficient because no further binding was found thereafter [5]. After incubation, the particles were separated from the solution by ultrafiltration. The quality of separation was estimated visually because of the rhodamine labeling of the particles. The free Gd^{3+} concentration in the permeate was determined by the arsenazo (III) assay. Although frequently used [3, 5, 12–14], this assay is known to be influenced by different environmental conditions. The results of reliability of the arsenazo (III) assay in different buffer systems are presented in detail in ESM 1 of the Electronic supplementary material. With some restrictions, the physiological HEPES, Tricine, and Tris(HCl) buffers can be used in combination with this assay.

The difference between the Gd^{3+} concentration which was added to the particle suspension and the free Gd^{3+} concentration yields the totally bound Gd^{3+} concentration. Directly, this concentration is accessible by using $^{153}GdCl_3$ and measuring the count rate of the γ radiation of the separated particles after incubation. The particles were separated and washed in buffer solution to remove unspecific bound Gd^{3+}. The amount of specifically bound Gd^{3+} was measured by determining the count rate of the particles after washing. Knowing the concentration of free, totally bound, specific, and unspecific bound Gd^{3+}, all concentrations are known that are needed to calculate binding parameters using well-known receptor/ligand approaches [15, 16].

An example of the preparation of colloidal stable Gd^{3+}-modified particles was given in [5]. The binding parameters and the maximum binding, however, were not determined. The following binding experiments were performed to investigate the conditions to obtain colloidal stable suspensions of Gd^{3+}-modified particles in more detail.

In first experiments, highly concentrated particle suspensions (≈5 wt.%) were mixed with $GdCl_3$, whereby no binding saturation could be achieved. At low particle concentration, the binding was faced with problems of colloidal stability. Figure 2a shows two examples of bound Gd^{3+} amount versus the Gd^{3+} concentration added for two constant particle concentrations. Obviously, the binding affinity of the particles in water is high. Nearly two thirds of the offered Gd^{3+} amount is bound by the particles. A saturation is not reached for a particle concentration of 0.5 wt.%. For a particle concentration of 0.05 wt.%, the suspension becomes colloidally instable at a Gd^{3+} concentration higher than 700 μg/mL. There is, however, another

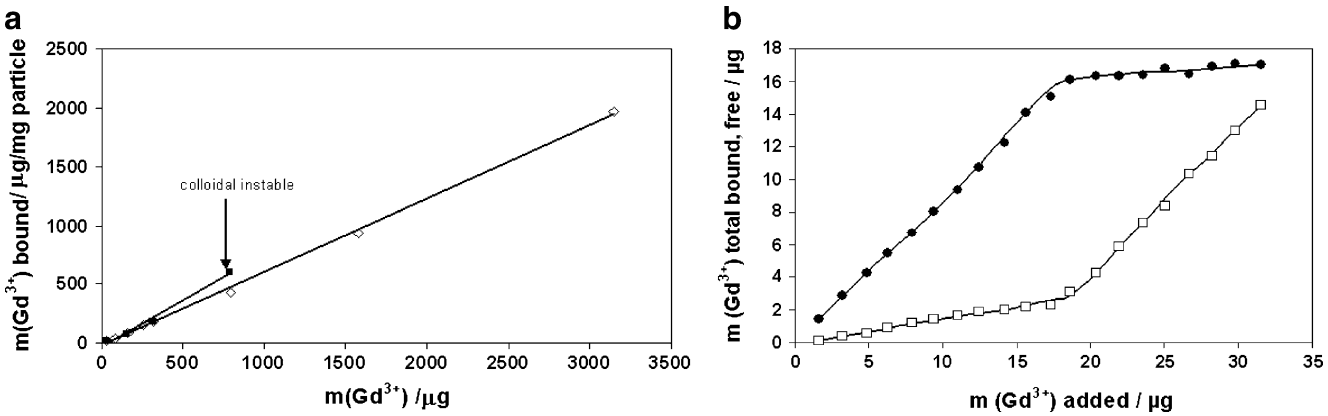

Fig. 2 **a** μg Gd^{3+} bound per mg particle versus amount of Gd^{3+} added to an aqueous CL3 particle suspension in μg. Particle concentration: 0.05 wt.% (■) and 0.5 wt.% (◊). **b** μg Gd^{3+} total bound (●) to CL3 particles and free (□) in the suspension versus amount Gd^{3+} added to an aqueous CL3 suspension in μg. Gd^{3+} bound was determined by the arsenazo (III) assay, room temperature. pH not adjusted

important aspect to be mentioned. The particles in the 0.05 wt.% suspension definitely bind the same or even more Gd^{3+} than those in the 0.5 wt.% suspension (Fig. 2a).

Figure 2b shows the dependence of both bound and free amounts of Gd^{3+} versus the Gd^{3+} amount added. The figure clearly demonstrates that the amount of free Gd^{3+} is always considerably smaller than the amount of bound Gd^{3+}. Therefore, Gd^{3+} depletion becomes evident because of the high binding affinity of the particles. A pronounced binding saturation plateau appears. The amount of both bound and free Gd^{3+} increases nearly linearly up to this saturation plateau. At concentrations exceeding the binding saturation, the amount of bound Gd^{3+} remains constant whereas that of free Gd^{3+} steeply increases.

The reason that the particles in the 0.05 wt.% suspension bind the same or even more Gd^{3+} than those in the 0.5 wt.% (Fig. 2a) becomes clear when the pH of the particle suspension is taken into account.

It is acidic and pH decreases with increasing particle concentrations. The pH value becomes 3.2 for a 3 wt.% CL3 suspension (Fig. 3). It is obvious that this strongly reduced pH in turn diminishes the binding capacity of the particles, which can be explained by changing the dissociation equilibrium of the carboxylic MAA residues at higher H^+ concentrations. This remarkably reduces the amount of Gd^{3+} binding.

There is a further aspect that may influence the heavy metal ion binding. Changes in pH are known to influence the particle corona, as mentioned above.

Figure 4 shows an example of this influence on the particle size of CL6 particles. The particle diameter decreases by about 30% when the environment becomes more acidic, which can be explained by corona compression such that the size approaches the size of the particle core. This effect definitely reduces the accessibility of the binding sites and decreases the binding capacity of the particles in acidic environment.

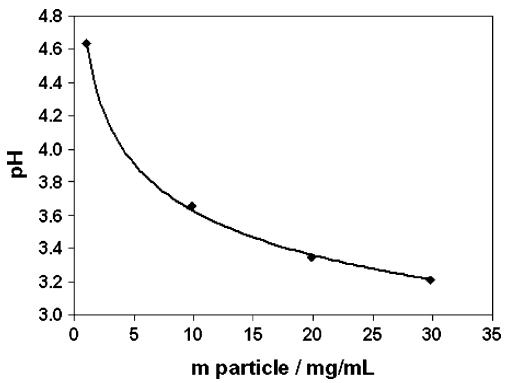

Fig. 3 Self-adjusting pH in water depending on the CL3 concentration

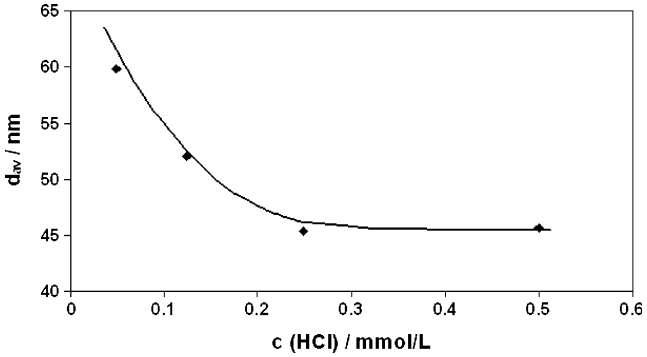

Fig. 4 Dependence of the particle size of CL6 versus the concentration of HCl added

Titration experiments with NaOH confirm that particles titrated to pH 7.4 show indeed a much greater binding capacity; see Fig. 5. When adding Gd^{3+} to such a pH-adjusted suspension, the pH however decreases again by Gd^{3+}/H^+ exchange. Therefore, promising binding experiments have to be carried out in buffered systems.

The Gd^{3+} incubation with the Tricine and HEPES buffer reveals differences in Gd^{3+} binding to the particles. More Gd^{3+} can be bound to the particles in HEPES than in Tricine (see Fig. 5).

This might be caused by either effects of the buffers on the particle shell or an interaction between Gd^{3+} and components of the buffer itself. It was found that Gd^{3+} addition indeed causes a small shift of the pH when Gd^{3+} was added to a 50mM Tricine buffer (data not shown), caused by the competition between Gd^{3+} and H^+ in Tricine buffer, which slightly decreases the Gd^{3+} amount bound. For binding studies, it is, however, important not to disturb the dissociation equilibrium. Therefore, an alternative method has been worked out to investigate binding of Gd^{3+} to particles in buffers.

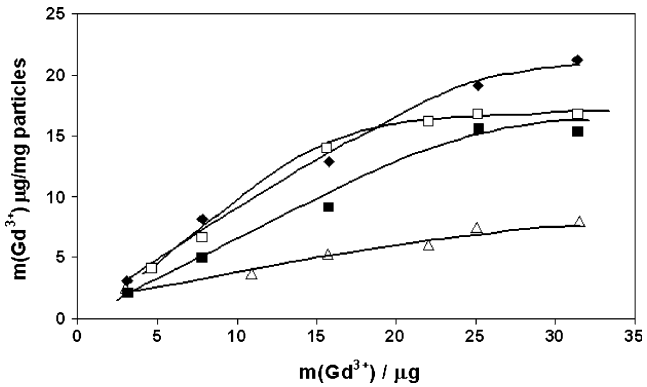

Fig. 5 Total binding of Gd^{3+} to CL3 particles in water (*open symbols*) and buffer solutions, pH 7.4. Δ self-adjusting pH in a 1 wt.% solution, □ pH titrated to 7.4 in water, ■ particles in Tricine buffer, and ♦ in HEPES. pH of the buffer solutions was adjusted to 7.4

Firstly, we titrated the particle suspension with NaOH to the pH of 7.4. A titration to higher pH is not useful, because at higher pH $Gd(OH)_3$ starts to form. The pH of a double concentrated buffer solution was adjusted to 7.2 and added to the particle solution (1:1). These conditions were found to guarantee a pH of about 7.4 within the range necessary for the binding experiments. Na^+ binds to the particles by titrating the suspension with NaOH. Gd^{3+} replaces both Na^+ and remaining H^+ after addition of the buffer solution and incubation of the suspension with $GdCl_3$.

This procedure was found to yield the highest amounts of Gd^{3+} binding to the particles in buffered solutions.

Figure 6 shows isotherms for total Gd^{3+} binding to CL3 particles, whereas the amount of bound Gd^{3+} was determined by both the arsenazo (III) assay, to measure the concentration of free Gd^{3+} after particle separation, and directly by radiochemical measurements, i.e., by incubation with $^{153}GdCl_3$ and measurement of the radioactivity of the particle pellet after ultrafiltration. The isotherms obtained using the arsenazo (III) assay are in good agreement with those found radiochemically.

Usually, the unspecific binding is determined radiochemically by competitive binding experiments. In these experiments, the binding of a single concentration of labeled ligand in the presence of various concentrations of unlabeled ligand is measured. That means that these experiments have to be performed in solutions with a high ligand excess [16, 17]. This, however, is not suitable for the case of Gd^{3+}-modified particles because, at Gd^{3+} concentrations higher than the binding saturation, the systems may become colloidally unstable. Therefore, another approach has to be used to determine unspecific binding. One possibility is to separate the Gd^{3+}-modified particles by ultrafiltration and to add a supplementary amount of buffer solution to wash the pellet, i.e., to remove unspecific bound metal ions. After repeated washing procedures and particle separation, the radioactivity can be determined of both the filtrated solution and the pellet, which corresponds to the unspecifically and specifically bound fraction.

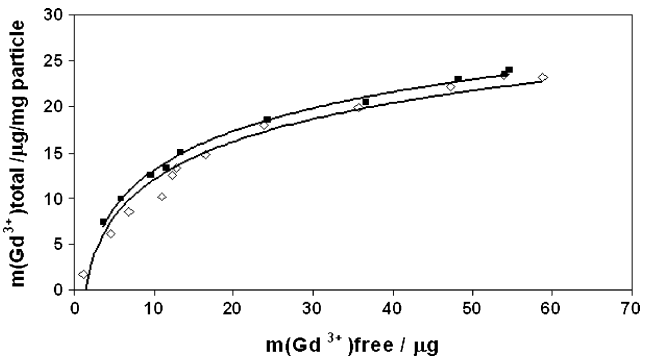

Fig. 6 Isotherm of total binding Gd^{3+} versus free concentration of G^{d3+} for CL3. Particles titrated to pH 7.4 and transferred into Tricine buffer (pH 7.4). Free concentration determined using the arsenazo (III) assay (■) and ^{153}Gd (◊)

Using this procedure, the following isotherms were obtained:

Usually, the unspecifically bound Gd^{3+} is expected to increase linearly with increasing free Gd^{3+} concentration. Here, this is obviously not fulfilled.

Comparison and prediction of binding data are not trivial for particles with different size and charge. The particle diameter is the only parameter that can be determined with acceptable accuracy. The EPMA/MAA ratio is known from the molar monomer concentrations and the fact that, after filtration, no free MAA is detected, i.e., the whole amount of MAA was involved in corona formation. For binding experiments, it is convenient to refer the binding amount, i.e., µg Gd^{3+}, to 1 mg of particle but actually not each part of a mg particle is involved in binding events to the same extent. The binding is determined rather by the particle surface and by the MAA groups which are expected to be accessible than by the whole particle mass. The surface of a large CL3 particle within a geometrical unit ($140\times 140\times 140$ nm^3) is about 2.3 times smaller than that surface realized by a corresponding number of CL6 particles (approx. eight particles), which fit into the same unit. When taking into account the molar ratio of 3.5 (EPMA/MAA 7:1 for CL3 and 2:1 for CL6) that counts for the different quantities of MAA groups per particle, one can expect that the eight CL6 particles could bind approximately eight times more Gd^{3+} than CL3 (Fig. 7). Actually, we find that CL6 binds only about twice as much as CL3. A calculation based on the assumption of rigid compact particles and the charge densities (see Table 2) clearly shows that the present particles decisively differ from such an idealized model. Both particles seem to differ strongly in the accessibility of the binding sites and therefore bind much less than expected from ideal considerations. Furthermore, the high density of negative charges on a surface unit of the particles may cause several other unexpected effects; the pH in the vicinity of the particle surface may be strongly reduced, which protonates the MAA groups. The particles may be extensively screened by counter ions, which also reduce the electrostatic interaction between the particles and Gd^{3+}. Obviously, a large amount of Gd^{3+} is attracted by the particles, but only a portion of about 65% for CL6 and 70% for CL3 is specifically bound, whereas about 35% or 30%, respectively, Gd^{3+} can be easily removed by a washing procedure. This means that a large amount of Gd^{3+} binds to the particles, whereas a considerable portion of these ions is only weakly bound.

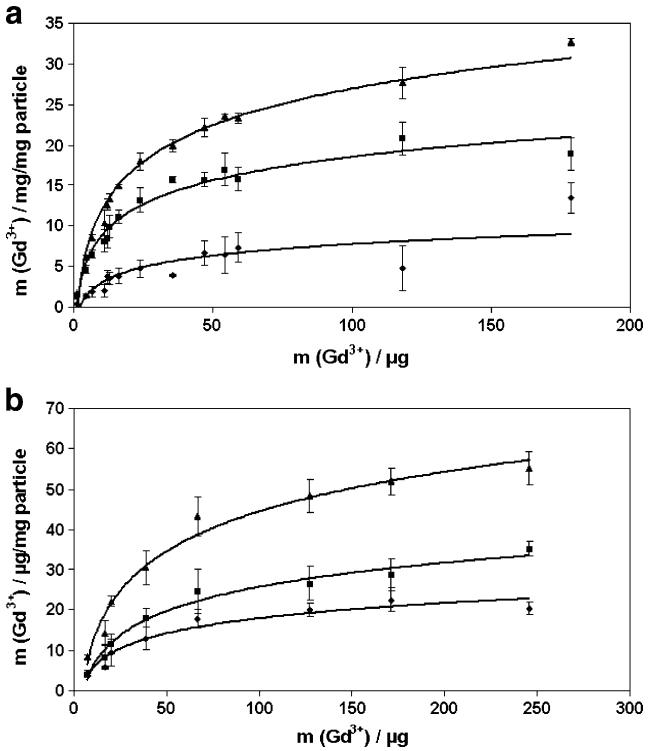

Fig. 7 Binding isotherms of CL3 (**a**) and CL6 (**b**) particles. Particle suspensions were titrated to pH 7.4 and transferred into Tricine buffer. ▲ Total binding, ■ specific binding, ♦ unspecific binding

Determination of the binding constants

There are different approaches to determine binding constants from bound and free amounts of ligand. Usually, these approaches assume that

- the binding follows the law of mass action and that the system investigated has been equilibrated,
- there is no partial binding,
- only a small fraction of the ligand binds, so that the free ligand concentration is nearly identical with the concentration added,
- binding is reversible, and
- binding of a ligand to one binding site does not influence the affinity of another binding site, i.e., there is no cooperativity and k_D remains constant during the experiment.

It is improbable that these conditions might be fulfilled for the case of interaction between Gd^{3+} and "hairy" particles with a high density of equally charged groups of receptor at the particle surface. As shown in Fig. 2, ligand depletion is definitely to be expected. As better approaches are not available, we use all common approaches regardless of the observance of the underlying prerequisites. It will be shown that the differences between the results are small, so that finally the results yield a crude impression of the real binding behavior.

The simplest approach is based on the Scatchard plot, i. e., a graph of bound ligand/free ligand versus bound ligand. This plot yields a linear dependence when there is only one binding site. In such a plot, B_{max} is the X intercept and k_D is the negative reciprocal value the slope, with k_D being the dissociation constant and B_{max} the maximum number of binding sites, not to be confused with the maximum amount of bound Gd^{3+}. There are a lot of problems with this approach, e.g., the linear transformation distorts the experimental error [18]. The error propagation between X and Y is altered, because errors of Y, i.e., the ratio Gd^{3+} bound/Gd^{3+} free, are also influenced by the errors of Gd^{3+} free. Nevertheless, this approach is used as ever. Although not expected, the Scatchard plot shows a linear dependence for both particles (see Fig. 8a) with a regression coefficient R^2 0.9366 for CL3 and 0.7957 for CL6. R^2 was determined by least-square analysis.

A better approach is the non-linear regression. To calculate the binding parameters, MathPad Prism 5.0 was used. It should be remembered that, for the non-linear regression, the same prerequisites are valid as specified above. Figure 8b shows the corresponding curves for the two particles. Clearly, the experimental data are also satisfactorily described by this approach.

As mentioned above, one prerequisite for binding experiments is that only a small fraction of the ligand binds and that the free concentration of ligands remains nearly unaffected by the binding. This is definitely not fulfilled for the case of binding between Gd^{3+} and the particles, as it was seen already from the first plots of binding data (see Fig. 2). Motulsky [15] stated that a difference of about 10% between the total amount of ligand and the free ligand concentration is tolerable. In the present case, the difference is much larger. Swillens [19] developed an alternative approach for such cases where a ligand depletion becomes remarkable. It uses a fit of total binding as a function of the added ligand with an equation that accounts both for non-specific binding and for ligand depletion. The paper shows [19] that fitting total binding gives more reliable results than would be obtained by calculating the free ligand concentration by subtraction. For calculation of the binding parameters, a non-linear regression is finally required, for which the MathPad Prism 5.0 program was used.

Beside these approaches, the Hill plot (Fig. 8c) is often used as this plot allows distinguishing cooperativity and non-cooperativity. This plot uses a graph $\log(B/B_{max}-B)$ versus $\log(Gd^{3+})$ free with B the current ligand concentration bound and B_{max} the number of maximum binding sites [16], which must be known from other experiments. Usually, this graph also yields lines. If the slope n_H of the straight lines equals 1, there is no cooperativity and the reaction between Gd^{3+} and the particles can be treated like

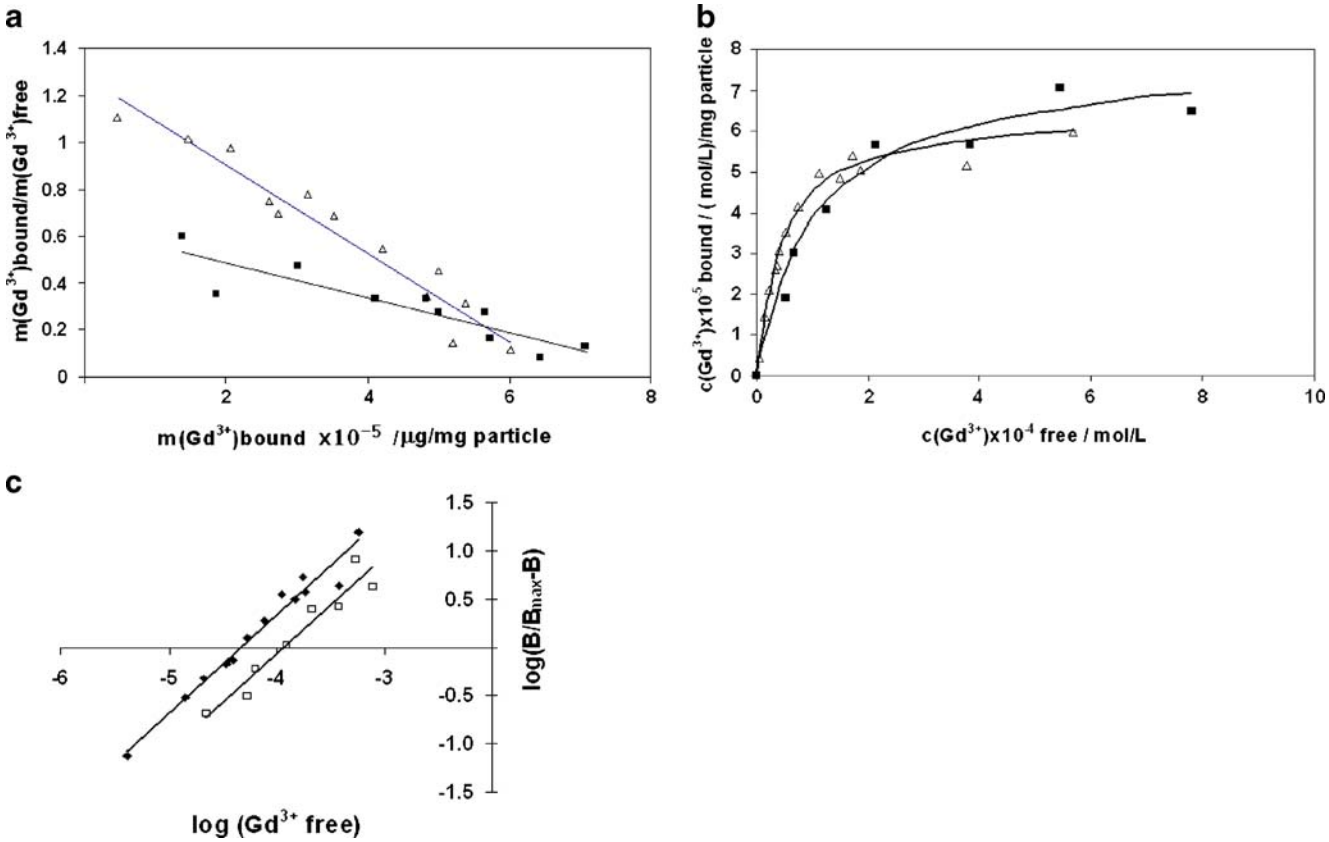

Fig. 8 Binding isotherms. CL3 (Δ) and CL6 (■). **a** Scatchard plot, ratio of the bound and free amount of Gd^{3+} versus bound amount. **b** Non-linear regression, concentration of specific bound Gd^{3+} per mg particle versus concentration of free Gd^{3+}. **c** Hill plot

a bimolecular reaction. Furthermore, the *X* intercept permits calculation of k_D. Table 3 summarizes all binding parameters determined. For the results of the Hill plot, the B_{max} values were used that were determined using the Swillens approach.

The relative good agreement between the parameters determined by different approaches is remarkable considering that all calculations can give only a crude approach to the binding behavior investigated. It should be noticed that the parameters that consider the ligand depletion appear between Scatchard and the non-linear regression.

In general, all dissociation constants $<10^{-3}$ mol/L indicate a strong binding. Therefore, the binding characterized has to be considered to be strong, although the k_D found are not comparable to chelate binding constants. Comparing the values of B_{max} of the two particles, it becomes clear that CL6 expresses only about 20% more binding sites for Gd^{3+} than the CL3 particles. The k_D of the CL3 particle is smaller than that of CL6. Therefore, CL3 binds Gd^{3+} more strongly than does CL6. Here, it should be considered that the results of the Scatchard plot and the non-linear regression are not influenced by any non-specific binding. Therefore, the difference between CL3 and CL6 in binding is better explained by the influence of the binding site arrangement at the particle surface and binding accessibility or particle surface pH value reduction than by effects caused by the Gd^{3+}, i.e., counterion screening, binding of Gd^{3+} to more than one particle.

Table 3 Comparison of the calculated binding parameters

	CL3			CL6		
	k_D mol/L	B_{max} mol/L	n_H	k_D mol/L	B_{max} mol/L	n_H
Scatchard	5.23×10^{-5}	6.75×10^{-5}	–	1.32×10^{-4}	8.65×10^{-5}	–
Non-linear regression	4.39×10^{-5}	6.35×10^{-5}	–	1.15×10^{-4}	7.97×10^{-5}	–
Swillens	4.74×10^{-5}	6.40×10^{-5}	–	1.20×10^{-4}	8.01×10^{-5}	–
Hill	4.51×10^{-5}	–	1.0153	1.17×10^{-4}	–	1.0021

The slopes of the Hill plot for both CL3 and CL6 are about 1 with only small deviations, i.e., coefficients of determination R^2 0.9675 for CL3 and 0.9283 for CL6, respectively. These results show that the reaction of Gd^{3+} binding to the receptors of the particles follows the law of mass action, that there is no cooperativity, and that the reaction between Gd^{3+} and the particles can be treated like a bimolecular reaction.

Characterization of the range of colloidal stability

Colloidal properties such as particle charge, size, and polydispersity are essential to prepare carriers for in vivo experiments. The parameters of the bare particles were reported above. In the following, the parameters of the Gd^{3+}-modified particles are presented in order to establish the range of colloidal stability of particle suspensions influenced by the presence of $GdCl_3$. The colloidal stability is more influenced by the ionic strength in the suspension than by the total binding. Consequently, problems of suspension stability usually occur at Gd^{3+} concentrations above the particle saturation, i.e., at concentrations exceeding B_{max}. In sufficiently concentrated particle suspensions, the range of colloidal stability is roughly easily judged because the precipitates are visible. In diluted systems, the range of colloidal stability can be determined more precisely by dynamic light scattering. Formation of particle aggregates of course affects the polydispersity, PDI. In practice, we prefer to determine the inset of colloidal instability by a small number of particle size measurements. Usually, the standard deviation in particle size measurements of homogeneous particles is low, but it strongly increases when aggregates occur and aggregates of different size start to be recorded.

Figure 9 shows the dependence of the particle size of CL3 on the concentration of free Gd^{3+} in pure water. Before loading with gadolinium, the particles were adjusted to a pH of 7.2 with NaOH leading to an exchange of sodium by gadolinium. This graph can be used as a criterion to judge the range of colloidal stability, which is important for particle in vivo application. There were no significant differences in size detected between the bare CL3 particles and those loaded with Gd^{3+} ions. In the range of colloidal stability, d_{av} remains constant. Data scattering is negligible. d_{av} increases remarkably when particle aggregation starts. Data scattering increases when the free Gd^{3+} concentration becomes larger than 12 μg and further increases almost linearly due to the effect of the ionic strength of Gd^{3+}, Na^+, and H^+. By the interception of the two straight lines, one characteristic for the range of constant particle size and the other in the range of increasing size, the concentration of particle aggregation can be more precisely determined than by the PDI.

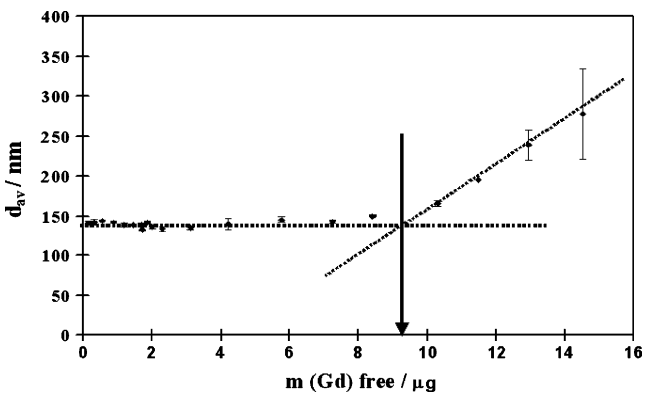

Fig. 9 Dependence of the average particle diameter of CL3 (1 mg/mL in water) on the free amount of Gd^{3+} in the suspension

Aggregation for "hairy" particles is caused by different effects: compression of the electrolytic double layer, but also ionic bridging, a binding of Gd^{3+} to more than one particle. The most prominent effect is compression of the ionic double layer at high ionic strength, which decreases the disjoining pressure between the particles, thus leading to aggregation.

Similar experiments were performed for CL6 particles. Table 4 presents the data of constant d_{av} for both particles in 50 mM Tricine buffer depending on the free concentration of Gd^{3+}. Tricine was used in these experiments because the buffer is physiological. There is a wide range of free Gd^{3+}, where particle aggregation does not occur, sufficient to select concentrations for preparing first solutions to access enhanced contrast for MRI imaging. The amount of Gd^{3+} needed for MRI experiments is adjusted after the loading procedure.

Visualization of particles and aggregates by AFM is given in ESM 2 of the Electronic supplementary material.

It should be noted that the present aggregation experiments cannot predict aggregation behavior in physiological

Table 4 Particle size and standard deviation depending on the concentration of free Gd^{3+} in 1 mg/mL suspensions (Tricine buffer)

Particle	m (Gd^{3+}) free μg	d_{av} nm	STD—standard deviation nm
CL3	0.22	141.5	±1.8
	3.58	143.0	±2.0
	5.77	143.6	±2.8
	9.44	144.3	±2.1
	11.68	144.5	±2.3
	16.42	144.5	±3.7
CL6	18.23	50.2	±0.4
	19.71	55.4	±0.5
	63.15	54.0	±1.3
	104.43	53.6	±2.0
	151.15	51.2	±1.0
	230.71	49.9	±1.3

liquids or even in blood. To judge such behavior requires more extended investigation to include particle/protein interaction. Such studies were not within the scope of the present study but are reserved for further investigation.

Summary

Two carboxylated P-EPMA nanoparticles were synthesized with different size and charge, i.e., 140 (CL3) and 60 nm (CL6) in diameter whereby the smaller particles had an EPMA/MAA ratio of 2:1 in contrast to the others with 7:1. Suspensions of these particles represented strongly negatively charged systems with both high binding affinity and capacity for cations, and were highly acidic, thus strongly reducing the pH of their suspensions. This behavior strongly determined the binding behavior with gadolinium cations. The binding affinity of the particles investigated was high, but the binding was strongly reduced in acidic environment by shifting of the dissociation equilibrium of the carboxylic surface functions of the MAA residues. Studies of binding behavior require constant pH conditions. The suitability of three physiological buffers had been investigated to establish the compatibility with the arsenazo (III) assay to determine the free Gd^{3+} concentration (see ESM 1 of the Electronic supplementary material). Two independent analytical methods were used to determine both the amount of free (arsenazo (III) assay) and bound (radiochemical) Gd^{3+} in the suspension separately. HEPES, Tricine, and Tris(HCl) buffer were compatible with the arsenazo (III) assay, whereas Tris(HCl) showed reduced analytical sensitivity. Binding results determined radiochemically and using the arsenazo (III) assay agreed when suitable buffered systems were used.

The best binding data were obtained when the particle suspensions were titrated firstly to pH 7.4 with NaOH, transformed into the buffer, and incubated with $GdCl_3$. Titration with NaOH caused partial Na^+ binding whereas Gd^{3+} replaced both Na^+ and remaining H^+ during incubation in buffered environment.

Binding isotherms were recorded for the total, specific, and unspecific binding of Gd^{3+} by the particles. The binding parameters were analyzed using linear regression (Scatchard plot) [20, 21], non-linear regression [22], a correction introduced by Swillens [19] for ligand depletion, and the Hill slope [16]. The binding studies confirmed the high binding affinity of the particle, so that ligand depletion became evident. The binding of Gd^{3+} to the particles was strong with binding constants $k_D \approx 10^{-4}$ mol/L for the smaller particles CL6 and $k_D \approx 5 \times 10^{-5}$ mol/L for the larger particles, CL3. Although the binding capacity of CL6, calculated by simple geometrical considerations, could be eight times higher than that of CL3, the CL6 particles bind only about 2.3 times more Gd^{3+}, which was confirmed by the maximum number of binding sites B_{max}. Knowing B_{max} and the amount of specifically bound Gd^{3+}, the fractional occupancy per particle could be calculated. Although the binding was 50% higher for CL6 in comparison with CL3, it is small when taking into account the 60% higher negatively charged surface of the larger particles. The small differences in B_{max} revealed that the accessibility of the MAA residues was strongly reduced when these groups are highly concentrated on a small area.

The Hill slopes determined indicated no cooperativity for the coupling between Gd^{3+} and the particles.

The suspensions became colloidally instable at sufficiently high Gd^{3+} concentrations, not far above the binding saturation, when the particle ionic double layer became compressed at high ionic strength. The onset of colloidal instability could be estimated in sufficiently diluted suspensions by using particle size measurements and was indicated by both an increase in particle size and an increase in data scattering, rather than by changes in the polydispersity index. Particle aggregates formed by deformed single particles could be visualized by AFM. The friction force determined by the lateral deflexion of the cantilever enabled the particle core and surrounding corona to be distinguished.

Knowing the range of colloidal stability and the maximal amount of bound Gd^{3+}, particle suspensions can be chosen to investigate the contrast-enhancing properties of these particles in MRI.

References

1. Lawaczeck R, Menzel M, Pietsch H (2004) Superparamagnetic iron oxide particles: contrast media for magnetic resonance imaging. Appl Organometal Chem 18:506
2. Caravan P, Ellison JJ, McMurry TJ, Lauffer RB (1999) Gadolinium(III) chelates as MRI contrast agents: structure, dynamics, and applications. Chem Rev 99:2293
3. Turner JL, Pan DPJ, Plummer R, Chen ZY, Whittaker AK, Wooley KL (2005) Synthesis of gadolinium-labeled shell-cross-linked nanoparticles for magnetic resonance imaging applications. Adv Functional Mater 15:1248
4. Vuu K, Xie JW, McDonald MA, Bernardo M, Hunter F, Zhang YT, Li K, Bednarski M, Guccione S (2005) Gadolinium-rhodamine nanoparticles for cell labeling and tracking via magnetic resonance and optical imaging. Bioconj Chem 16:995
5. Cartier R, Kaufner L, Paulke BR, Wüstneck R, Pietschmann S, Michel R, Bruhn H, Pison U (2007) Latex nanoparticles for multimodal imaging and detection in vivo. Nanotechnology 18:195102
6. Wang RB, Schmiedel H, Paulke BR (2004) Isothermal titration calorimetric studies of surfactant interactions with negatively charged, 'hairy' latex nanoparticles. Colloid Polym Sci 283:91
7. Zyryanov AB, Baykov AA (2002) Biochemistry (Moscow, Russ. Fed.) 67:635
8. Paulke B-R, Möglich P-M, Knippel E, Budde A, Nitzsche R, Müller RH (1996) Electrophoretic 3D-mobility profiles of latex particles with different surface groups. Langmuir 11:70

9. Kubaska S, Sahani DV, Saini S, Hahn PF, Halpern E (2001) Dual contrast enhanced magnetic resonance imaging of the liver with superparamagnetic iron oxide followed by gadolinium for lesion detection and characterization. Clin Radiol 56:410
10. Geiser M, Rothen-Rutishauser B, Kapp N, Schurch S, Kreyling W, Schulz H, Semmler M, Hof VI, Heyder J, Gehr P (2005) Ultrafine particles cross cellular membranes by nonphagocytic mechanisms in lungs and in cultured cells. Environ Health Perspect 113:1555
11. Ohshima H (2007) Electrokinetics of soft particles. Colloid Polym Sci 285:1411–1421
12. Nagaraja TN, Croxen RL, Panda S, Knight RA, Keenan KA, Brown SL, Fenstermacher JD, Ewing JR (2006) Application of arsenazo III in the preparation and characterization of an albumin-linked, gadolinium-based macromolecular magnetic resonance contrast agent. J Neurosci Methods 157:238
13. Gouin S, Winnik FM (2001) Quantitative assays of the amount of diethylenetriaminepentaacetic acid conjugated to water-soluble polymers using isothermal titration calorimetry and colorimetry. Bioconj Chem 12:372
14. Kijkowska R (2004) Effect of Ca on gadolinium phosphate crystallisation from phosphoric acid solution. J Mater Sci 39: 2017
15. Motulsky H, President GS http://www.graphpad.com 1995/96, The GraphPad Guide to Analyzing Radioligand Binding Data
16. McKinney M, Raddatz R (2006) Practical aspects of radioligand binding. In: Enna SJ, Williams M, Ferkany JW, Moser P, Ruggeri B, Barrett JF, Porsolt RD, Sullivan JP (eds), Current protocols in pharmacology Vol. 1.3.1–1.3.42, Supplement 33, Wiley, New York. http://www.mrw.interscience.wiley.com/emrw/9780471141754/cp/cpph/toc
17. Motulsky HJ http://www.graphpad.com 1999, The GraphPad Guide to Analyzing Radioligand Binding Data
18. Rodbard D, Munson PJ, Thakur AK (1980) Quantitative characterization of hormone receptors. Cancer 46:2907
19. Swillens S (1995) Interpretation of binding curves obtained with high receptor concentrations: practical aid for computer analysis. Mol Pharmacol 47:1197
20. Rubinow SI, Segel LA (1991) Fundamental concepts in biochemical reaction theory. In: Segel LA (ed) Biological kinetics Cambridge University Press, Cambridge, p 1
21. Rosenthal HE (1967) A graphic method for determination and presentation of binding parameters in a complex system. Anal Biochem 20:525
22. Motulsky HJ (1999) Analyzing Data with GraphPad Prism; GraphPad Software, Inc